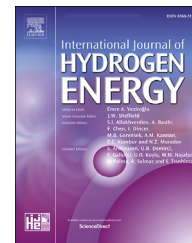




ELSEVIER

Available online at [www.sciencedirect.com](http://www.sciencedirect.com)

ScienceDirect

journal homepage: [www.elsevier.com/locate/he](http://www.elsevier.com/locate/he)

# Raman spectroscopy for ortho-para hydrogen catalyst studies

B. Krasch <sup>a,\*</sup>, S. Mirz <sup>a</sup>, A. Smolinski <sup>b</sup>, O. Süß <sup>b</sup>, R. Größle <sup>a</sup><sup>a</sup> Institute for Astroparticle Physics (IAP), Tritium Laboratory (TLK), Karlsruhe Institute of Technology (KIT), Hermann-von-Helmholtz-Platz 1, 76344 Eggenstein-Leopoldshafen, Germany<sup>b</sup> Institute for Technical Thermodynamics and Refrigeration (ITTK), Karlsruhe Institute of Technology (KIT), Hermann-von-Helmholtz-Platz 1, 76344 Eggenstein-Leopoldshafen, Germany

## HIGHLIGHTS

- Raman based measuring system to study ortho-para cryo catalyst kinetics.
- Raman method is independent of parameters, such as temperature, pressure, flow.
- Experimental setup with a closed hydrogen loop and cyclical operation down to 77K.

## ARTICLE INFO

### Article history:

Received 3 November 2022

Received in revised form

23 March 2023

Accepted 30 March 2023

Available online xxx

### Keywords:

Ortho-para hydrogen

Cryo catalysis

Raman spectroscopy

Direct ortho-para measurement

Monitoring

## ABSTRACT

For the design of efficient hydrogen liquefaction plants and for the production of accurate ortho-para hydrogen samples, precise knowledge about the kinetics of ortho-para catalysts and accurate ortho-para monitoring is mandatory. Raman spectroscopy as a direct measurement of the ortho-para ratio is independent of other gas parameters, such as temperature, pressure, and flow rate and also undisturbed by impurities, such as nitrogen and oxygen in the gas. Therefore, Raman spectroscopy is a superior technique for ortho-para monitoring, compared to methods based on thermodynamic properties like heat conductivity. Within this work, an experimental proof of concept of a Raman based system to study ortho-para catalyst kinetics is shown.

© 2023 The Authors. Published by Elsevier Ltd on behalf of Hydrogen Energy Publications LLC. This is an open access article under the CC BY-NC-ND license (<http://creativecommons.org/licenses/by-nc-nd/4.0/>).

## Introduction

Hydrogen has a central role in solving the challenge of a clean and affordable energy supply [1,2]. It can be used for energy storage, transport and as a zero-emission fuel [3–6]. Hydrogen, as well as its isotopes deuterium and tritium, are also of major interest in other applications and in

fundamental research. In fusion reactors, tritium and deuterium will be fused and the released energy is converted into electric power. In cold and ultra cold neutron sources for material and fundamental particle physics research, liquid and solid hydrogen and deuterium are used as moderators [7].

For us, the nuclear spin isomers, para and ortho hydrogen [8,9], are systematic effects in all kinds of research at the Tritium Laboratory Karlsruhe, e.g. it influences the so called

\* Corresponding author. Institute for Astroparticle Physics (IAP), Tritium Laboratory Karlsruhe (TLK), Germany.

E-mail address: [bennet.krasch@kit.edu](mailto:bennet.krasch@kit.edu) (B. Krasch).

<https://doi.org/10.1016/j.ijhydene.2023.03.461>

0360-3199/© 2023 The Authors. Published by Elsevier Ltd on behalf of Hydrogen Energy Publications LLC. This is an open access article under the CC BY-NC-ND license (<http://creativecommons.org/licenses/by-nc-nd/4.0/>).

final state distribution of the Karlsruhe Tritium Neutrino (KATRIN) experiment [10,11]. It is a major systematic effect in using IR absorption spectroscopy of liquid hydrogen isotopologues ( $Q_2 = T_2$ , DT, HT,  $D_2$ , HD,  $H_2$ ) as an analytic tool [12–15] and in the study of molecular dimers [16]. Besides this, ortho and para hydrogen differ in their boiling points and can be separated by cryogenic distillation and can therefore influence the performance of hydrogen isotope separation [15,17]. For these reasons, we were aiming to develop an analytic tool to enable accurate ortho-para measurement and manipulation to study its influence on the above mentioned experiments.

For the application of hydrogen as an energy vector, the low energy density at room temperature and ambient pressure is a major drawback. To increase the volumetric energy density, metal hydrides can be used at the cost of increased mass. Another solution is to liquefy the hydrogen at temperatures around 20 K [18–20]. For this, large-scale hydrogen liquefaction plants are used and are under ongoing development [21,22].

The main drawback of the liquefaction is the high energy consumption of this process. At the moment three major contributions to the avoidable in the liquefaction process have been identified: The primary cooling medium [23], the heat exchanger [24] and the ortho-para equilibration [21,25,26].

Since the hydrogen nuclei are spin-1/2-particles, they follow the Fermi-Dirac statistic and therefore the two nuclear wave functions have to form a fully antisymmetric superposition [27,28]. Ortho- ( $H_2$ ,  $D_2$ ,  $T_2$ ) is a fully symmetric nuclear spin triplet. The para modification is a fully antisymmetric nuclear spin singlet. To preserve the symmetry of the wave function, nuclear spins of ortho states are coupled with symmetric rotational states ( $J = \text{odd}$ ) and para with antisymmetric states ( $J = \text{even}$ ). Natural conversion between even and odd rotational states is strongly suppressed since the nuclear spins and the rotational state need to be switched at the same time [29].

At high temperatures, the ratio of the sum of even states (para) versus the sum of odd states (ortho) asymptotically reaches a ratio of 1:3. At the low temperature equilibrium, all molecules are in the rotational ground state ( $J = 0$ , thus para state). When cooling down hydrogen from high temperatures, the slow conversion process between ortho and para (due to the coupling of the nuclear spin and the rotational states) cause almost 75% of molecules to remain in the  $J = 1$  state, corresponding to the ortho state of  $H_2$ .

The ortho-para conversion process is mainly based on the interaction of the magnetic moment of the nucleus with a magnetic moment caused by neighbouring molecules (natural conversion) or by catalyst materials [30]. Even in the liquid phase, where the neighbouring molecules are very close together, it is still a slow process with time constants on the order of days [31–33].

By this, freshly liquefied hydrogen releases energy up to 520 kJ kg<sup>-1</sup> with a time constant of days [34], which exceeds the evaporation enthalpy 448.6 kJ kg<sup>-1</sup> [35]. Therefore, this energy release is a main design criterion for liquefaction processes and storage.

Thus, for the efficient technical scale liquefaction of hydrogen for storage and transport [36], the ortho-para conversion has to be forced during the liquefaction process [37–40]. For the ortho-para conversion, dedicated cryo

catalyst materials are needed [41]. Recent studies show, that 29% of the exergy destruction during the whole liquefaction process is due to the ortho-para conversion [24]. This demonstrates the high potential and impact of an optimised catalyst material and accurate catalyst data.

So far, previous experiments were based on the fact that ortho and para hydrogen have different thermodynamic properties which can be used as indirect measures of the ortho-para ratio [32,42,43]. Within this work, we demonstrate a new approach for the characterisation of cryo catalysts using Raman spectroscopy. Raman spectroscopy can directly measure the occupation of the rotational states and by this, the ortho-para ratio.

## Experimental method

The aim is to characterize the kinetics of the ortho-para conversion in dependence of the catalyst material and physical quantities such as temperature, pressure, and flow rate. Therefore, the catalyst material is filled into a converter tube which can be cooled down to 77 K or heated up to 673 K. Gaseous hydrogen is pumped in a closed loop through the catalyst and the Raman measurement cell which is at room temperature.

Since the natural conversion is much slower than the catalysed conversion, the ortho-para ratio can be assumed to be constant during cool down and heat up of the gas outside of the catalyst. This is illustrated in Fig. 1. The first row, labelled with a), corresponds to the room temperature distribution of the rotational states. Then the gas is quickly cooled down to 77 K while the ortho-para ratio stays constant, see b). When the gas interacts with the catalyst, the equilibration process starts and during each cycle through the catalyst the distribution changes only a bit. The full conversion from what is shown in b) to the distribution in c) is only reached after several cycles through the whole loop. In the long run the distribution will reach the cold equilibrium. Beyond the catalyst the gas is heated back to room temperature and after several cycles the rotational distribution, as shown in row d), is reached.

The amount of catalyst is chosen such that only a small fraction of the gas is catalysed during each cycle, but still significantly more is converted than by natural conversion alone. This gives enough time to cool down or heat up the catalyst and the heat generated by the ortho-para conversion in the catalyst can be assumed to be removed perfectly. In addition, this allows to assume that the ortho-para ratio of all gas inside the cycle is almost identical at any given moment and systematics, like back diffusion, can be neglected.

In this manner, the ortho-para ratio can be monitored accurately with the Raman system by measuring the rotational states' population is then a direct measure of the catalytic dominated conversion rate.

## Setup & measuring procedure

The experimental setup consists of a closed hydrogen loop, consisting of a converter filled with the catalyst, a laser Raman

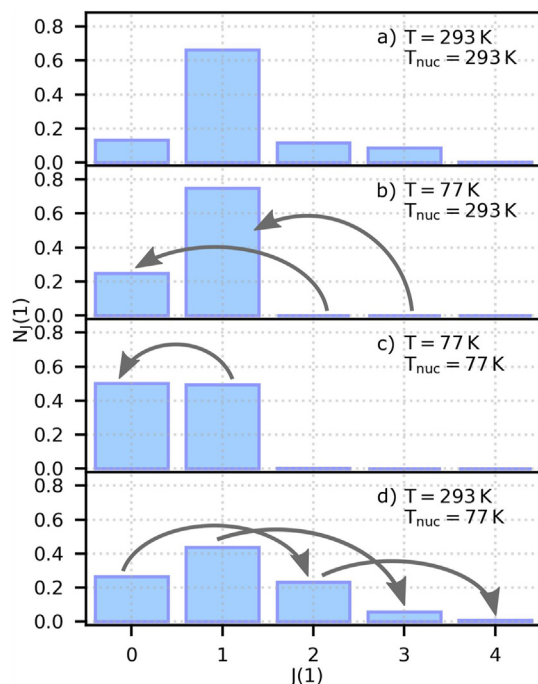


**Fig. 1** – Occupational numbers  $N_j$  of the rotational states  $J$  in a thermal cycle. Where  $T$  is the gas temperature and  $T_{\text{nuc}}$  is the corresponding temperature for the ortho-para equilibrium. Arrows indicate the net transfer of molecules from one state to another during each step. a)  $N_j$  and ortho-para at the 293 K equilibrium. b) Cool down with constant ortho-para ratio corresponding to  $T_{\text{nuc}} = 293$  K. c)  $N_j$  and ortho-para equilibrium at  $T_{\text{nuc}} = 77$  K. d)  $N_j$  at 293 K with the ortho-para equilibrium of  $T_{\text{nuc}} = 77$  K.

system to measure the ortho-para composition, a circulation pump, and sensors for pressure, temperature, and flow measurement and regulation.

### Converter

The converter (see Fig. 2) consists of three u-shaped stainless steel pipes connected in row, that can be put into liquid nitrogen for cooling or heated up for activation to increase the catalytic performance. The central pipe contains the catalyst material and two Pt-100 temperature sensors for gas temperature measurement which are installed 1 cm above the catalyst material. On the exterior surface of the central pipe heaters and thermocouples are installed. The heaters are used during activation of the catalyst. For the current proof of concept,  $\text{Fe}_2\text{O}_3$  was chosen since it is commonly used and therefore a good reference for our new approach. Specifically, 18g iron(III)-oxide from Sigma Aldrich,<sup>1</sup> milled and sieved to a grain size between 0.7 mm and 1.1 mm.

### Process gas system

An overview of the system is given in Fig. 3. We use  $\text{H}_2$  as process gas for catalyst activation and the ortho-para

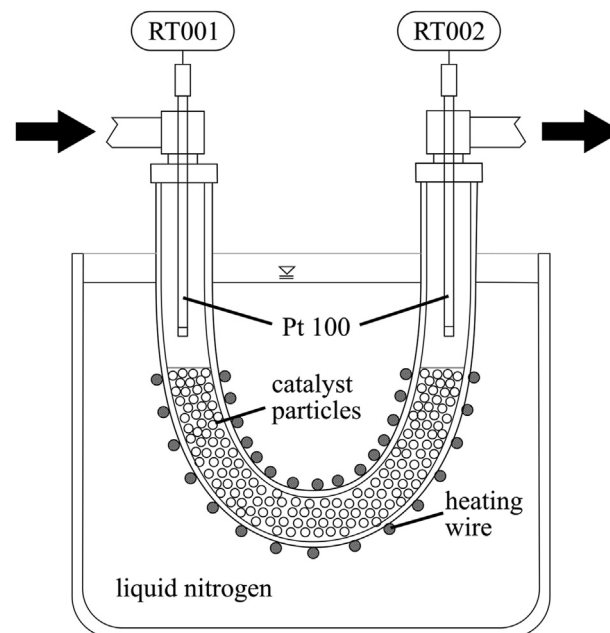


**Fig. 2** – Scheme of the converter. The converter can be filled with different catalyst materials.

conversion measurements. The pressure sensors and one buffer vessel ( $\approx 1$  L) are used to regulate the total gas pressure. The flow controller regulates the amount of gas streaming through the facility. The laser Raman cell (labelled LARA), the buffer vessel and the catalyst can be bypassed for cleaning, flushing and alternative operation modes. A turbo molecular pumping train evacuates the system to the  $10^{-6}$  mbar regime, which is used for catalyst activation and system cleaning. However due to the long pipes and the relatively large surfaces, it is not expected that his vacuum level is reached in the whole system so this needs to be combined with purging and heating to sufficiently clean the system.

### Laser Raman system

Raman spectroscopy is sensitive to rotational and vibrational excitations [44]. The Raman spectrum of a diatomic molecule consists of rotational branches of spectral lines grouped into vibrational bands. Inside of a rotational branch, each spectral line corresponds to a certain initial rotational state. The integral intensity of each line is proportional to occupational number and other parameters such as density, transitional matrix elements and overall system specific response functions. The transitional matrix elements are specific for each rotational state but only differ by less than a few percent [45] for Raman scattering. In addition, the spectrometer, detector and optics response functions are wavelength dependent. Therefore a calibration is needed for accurate measurements [46–49], which is achieved by measuring at a known ortho-para ratio. By this, the response function and the matrix elements are cancelled out. The density vanishes by normalizing to the calibrated sum so that we receive relative concentrations for each rotational state. Since we are mainly interested in the ortho-para ratio and not in the single

<sup>1</sup> registered office: St. Louis, Missouri, United States of America.

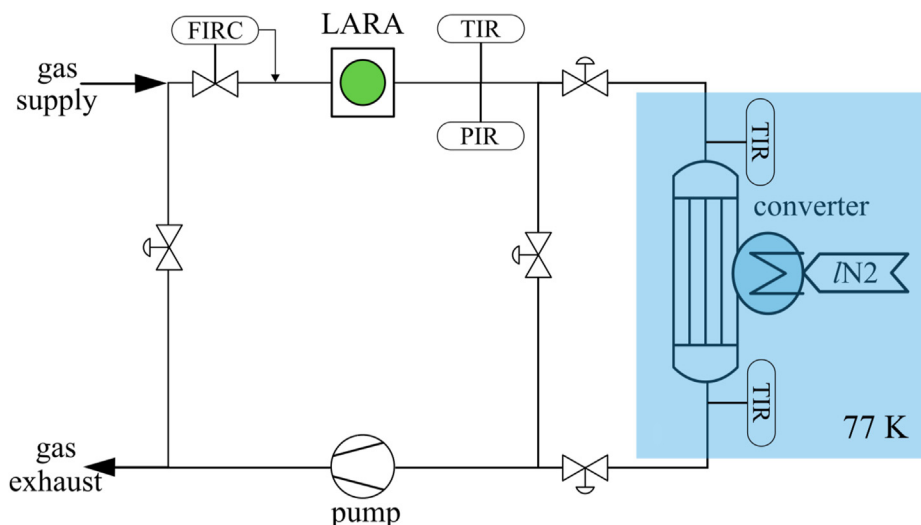


**Fig. 3** – Schematic flow chart of the experimental setup. TIR: Temperature Indicator and Recorder, PIR: Pressure Indicator and Recorder, FIRC: Flow Indicator, Recorder and Controller.

rotational states, the ortho fraction of the gas composition is then given by the sum of the occupational numbers of odd rotational states.

For those interested in the spectroscopic details; in the current setup we use the  $Q_1$  branches, where  $Q$  stands for zero rotational and 1 for one vibrational excitation (going from 0 to 1). Thus the  $Q_1(0)$  stands for the pure vibrational excitation of the rotational ground state. The labelling for the excitation of the rotational state  $J$  is then labelled with  $Q_1(J)$ . Fig. 4 shows the pure vibrational spectra of  $H_2$  at room temperature for the cases of the ortho-para ratio corresponding to room temperature and 77 K. Around room temperature and below, it can be assumed that all molecules are in the fundamental vibrational

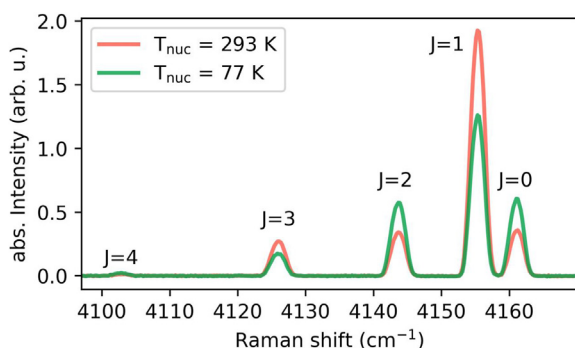


**Fig. 4** –  $Q_1$  branch of the Raman spectrum of pure  $H_2$  at room temperature (293 K) and two different ortho-para ratios. The absolute measured intensities as a function of the Raman shift are given, where each peak corresponds to one rotational state. The red line shows the spectrum at room temperature 293 K ortho-para equilibrium and the green line the spectrum for 77 K ortho-para equilibrium. The intensity of the even  $J$  states increases and for the odd states decreases as expected from Fig. 1. (For interpretation of the references to colour in this figure legend, the reader is referred to the Web version of this article.)

state  $\nu = 0$ . Therefore, the rotational quantum number  $J$  fully describes the molecular state. The analysis software for processing the taken Raman data is in-house development [48]. The basic analysis steps from the raw spectrum to the intensity spectrum are (see Fig. 4): dead pixel removal, cosmic ray removal, astigmatism correction, baseline subtraction, peak fitting, relative intensity calculation. The theoretical values for the transitional matrix elements are part of the last step.

### Measuring procedure

$H_2$  is fed into the system and circulated for several minutes at room temperature. The ortho-para ratio then corresponds to room temperature equilibrium and is monitored continuously at a frequency of one measurement per minute. Next, the converter is cooled down with liquid nitrogen to 77 K, to start the conversion process. The gas mixture circulates several times through the system until the ortho-para equilibrium is reached. During the whole conversion process, the liquid nitrogen level is always controlled and kept high enough by refilling with fresh liquid nitrogen. Two sensors monitor the temperature, see Fig. 3. In the next step, the converter is warmed up again to room temperature while the gas is still circulating.

To summarize, the circular approach allows us to measure the time evolution of the ortho-para ratio which is a direct measure for the catalyst performance. This is comparable to the information one gets from single pass experiments where hydrogen is sent only once through the catalyst and the performance is measured by the release of heat, the change in sound velocity, heat conductivity or other thermodynamic properties.

In addition to this, we can also derive information about the reaction order and the final equilibrium state. Using Raman spectroscopy, we can directly measure the ortho-para ratio instead of relying on a change in of thermodynamic properties, such as heat capacity, velocity of sound etc. Therefore, it will be also possible to mix in impurities like



nitrogen, oxygen, helium, or other gases to study in situ the influence of catalyst poisoning.

## Experimental proof of principle

The goal of the experimental campaign described in this contribution is to demonstrate the capabilities of this measurement principle.

### Preparation

Before the first measurement, the system had to be cleaned in order to remove impurities, such as nitrogen, oxygen, water etc. that might influence the reaction kinetics of the catalyst. For this, the setup was first evacuated below the millibar regime. Then it was filled with hydrogen (purity  $5.3 = 99.9993\%$ ) at 100 mbar which was then circulated through the system for up to an hour. This has been repeated several times. The catalyst itself was activated by heating to 120 °C for three days and continuously evacuated with a pumping train including a turbo molecular pump. Then, the system was flushed with hydrogen again and evacuated again below the millibar regime. Afterwards the system was filled with pure hydrogen to a pressure of 700 mbar as can be seen in Fig. 5b.

### Measurement

All valves were opened and the circulation pump started to provide a circular flow through the catalyst, Raman cell, flow meter, etc. The buffer vessel was excluded from the circulation to reduce the back-mixing of the sample. For the main part of the campaign, the catalyst was alternately cooled down to liquid nitrogen temperature for the time slot between 1124 min and 1204 min in Fig. 5 and heated back up again to room temperature to change the thermodynamic equilibrium of the ortho-para ratio. The measurement was always running for several half-life time constants of the ortho-para conversion in order to ensure reaching the temperature dependent equilibrium. This was then repeated several times. During the whole measurement the Raman cell, the flow meter, the buffer vessel, and the circulation pump were always at room temperature.

### Data analysis

The intensities of the Raman spectral lines corresponding to the  $J = 0, 1, 2, 3, 4$  rotational states were monitored with Raman spectroscopy. The ortho-para ratio was extracted from this by adding up the occupation number  $n$  of the even and the odd states respectively (Fig. 5d). Since the intensities are also sensitive to the molecular density, they are normalised to the sum of the intensities to extract the relative ortho-para ratios that are shown in Fig. 5e). The relative ortho fraction is given by

$$x_0 = \frac{\sum n_{j=\text{odd}}}{\sum n_{j=\text{odd}} + \sum n_{j=\text{even}}} \quad (1)$$

The time dependent ortho-para ratio can then be fitted with an exponential function  $f(t) = a + b \cdot \exp -t/\tau$  and the time constant  $\tau$  is a direct measure of the conversion rate and the catalyst activity. Only those data points were used when the converter had reached 77 K. The data points during the cooling process are not included in the fit.

### Exemplary results

In the given example in Fig. 5, the extracted time constants were  $\tau_{\text{cold}} = 6.8$  min and  $\tau_{\text{warm}} = 94.4$  min. The achieved relative concentrations for the cold and warm phase were then respectively  $c_{\text{ortho, cold}} = 0.501$  and  $c_{\text{ortho, warm}} = 0.755$ . This is within the expectation for the corresponding temperature and the overall accuracy of the Raman system. However, especially the total accuracy of the system will need further investigation since at the moment, we assume to be limited due to the calibration trueness and not due to the precision of the system. So further improvements here are possible.

Besides the shown example, several runs had been done to have a first exploration of the capabilities and limitations of the experimental method. In these tests, it was found that after proper activation of the catalyst, the repeatability of the time constants was already better than 10%. Deviations from the activation procedure in time, temperature, and flushing will lead to different catalytic activities. For example, when the activation time was too short the catalytic activity increased with following experiments since the hydrogen flushing even at room temperature could further improve the catalytic activity. However, this will need further and detailed investigation for each catalyst.

Also, a novelty compared to other measurement methods is that we are able to give time constants for the back conversion at room temperature which is possible due to the circular approach. This gives deeper insight into the underlying conversion process. In the case of iron oxide, theory predicts that the ortho-para conversion is based on physisorption of the molecule on the surface. This process is more effective at lower temperatures which is in agreement with time constants we found ( $\tau_{\text{cold}} = 6.8$  min,  $\tau_{\text{warm}} = 94.4$  min). Slower conversion at room temperature, quicker at liquid nitrogen temperature.

In addition, some prior investigations were done using palladium, which is known to be a good chemical catalyst. Palladium is used on a regular basis in our lab to partially convert  $\text{H}_2$ ,  $\text{D}_2$ ,  $\text{T}_2$  mixtures into HD, HT or DT. Typically, this catalysis process is done above room temperature since the catalysis process involves splitting the molecules which needs energy and therefore is more effective at high temperatures. As a consequence of splitting and recombining molecules, this chemical catalysis also serves as an ortho-para catalysis. Our measurements with palladium have shown that the ortho-para conversion is quicker at room temperature and slower at liquid nitrogen temperature. This fits the expectation from the theory that the chemisorbing process has the opposite temperature dependency of the physisorbing process. Further and detailed investigation of this is promising and can deliver detailed insight of the underlying catalysis process.

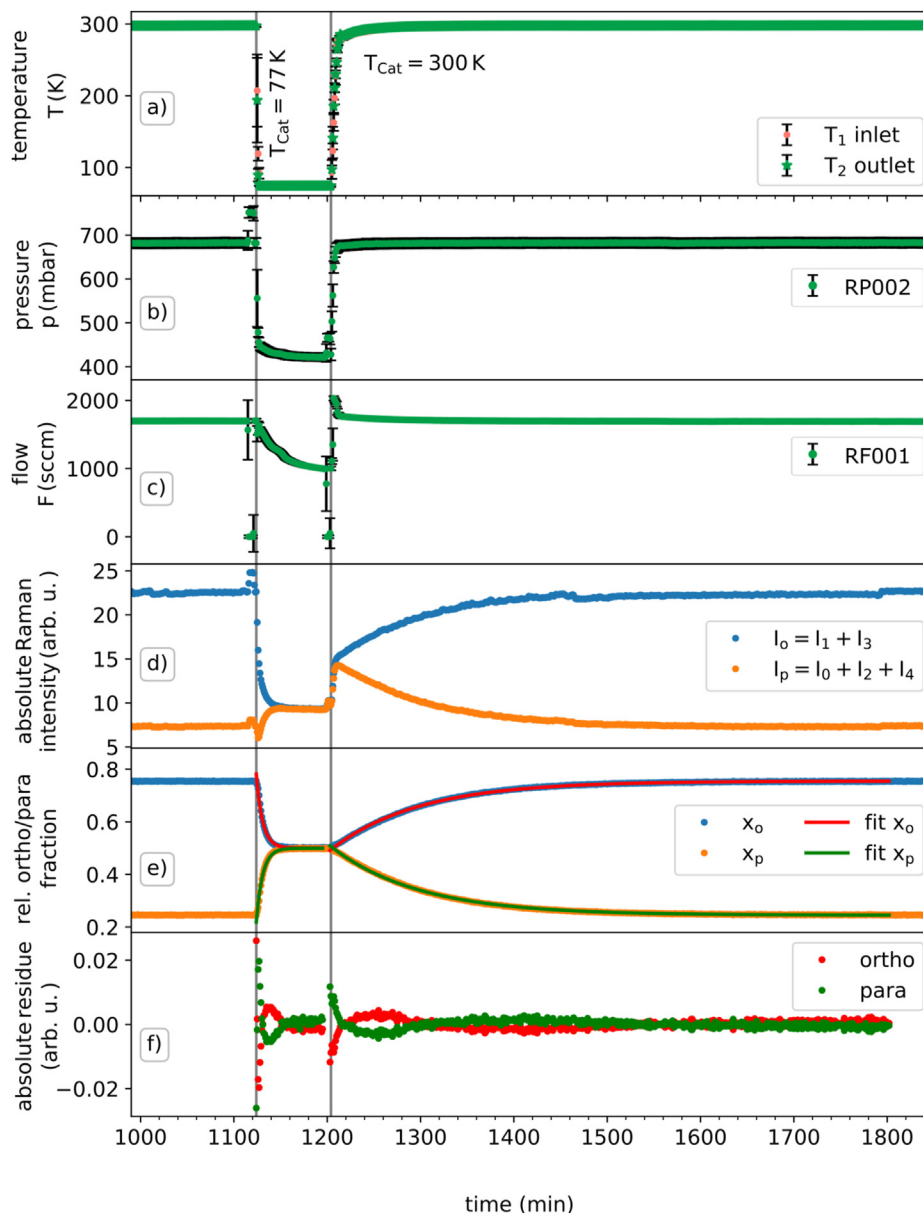


**Fig. 5 – RUN036: exemplary measurement cycle of ortho-para conversion of pure hydrogen.** It is shown one full cold warm cycle of the ortho-para conversion. As a function of the time, the parameters temperature  $T$ , pressure  $p$  and flow rate  $F$  and the Raman intensities  $I_0, I_1, I_2, I_3$  and  $I_4$  are measured. From  $I_{0,1,2,3,4}$ , the summed ortho and para intensities  $I_o$  and  $I_p$  are calculated. From this, the relative the ortho  $x_o$  and para  $x_p$  fractions are derived. For the relative fractions also, the best fits are shown. To give accuracy on the fits, the absolute residue, difference between the value obtained by the exponential fit and the measured value, are displayed.

## Systematics

The impact of systematic effects on the determination of the ortho-para ratio is crucial, since there are effects that can change the conversion rate by orders of magnitude.

### Natural conversion and level of detection

The first effects that always have to be considered are the auto catalysis of the hydrogen and a system-dependent catalysis due to the unavoidable experimental rig surfaces. For this, we

measured without catalyst and checked the auto catalysis rates and found that those effects are more than 50 times slower than the catalytic enhanced process. However, for further improvements of the accuracy, this will need detailed investigation.

### Raman spectroscopy

Raman spectroscopy has three main advantages over other methods. The intensities of the spectral lines scale linearly with the corresponding ortho or para concentration. Also, line strength functions for each line are very close to each other so

the intensities can be directly used to estimate the ortho-para ratio on a percent level [45]. An improvement in the accuracy, especially the trueness, is possible with a line by line calibration and is foreseen for the future. We are looking for the time constant  $\tau$  of the exponential evolution which is independent of the calibration. However, for higher precision, the calibration of the Raman system can be done with a hydrogen sample in the room temperature equilibrium. Measuring the intensities and comparing those to the calculated equilibrium [50], directly allows to derive the calibration constants for each line. Additionally, with the direct ortho-para measurement we gain even more information e.g., from the equilibrium state itself. This enables the direct identification of deviations in the equilibrium state due to temperature change or physical effects on the catalyst like ab-, de- or chemisorption processes [51].

### Temperature

There are three temperature sensors located in the setup (see Fig. 2), one at the entrance and one at the exit of the converter, and another one at the Raman cell. In the presented measurement campaign, the cooling to 77 K took approximately 6 min and the warming up to room temperature (293 K) took approximately 10 min. During these unstable temperature phases, the determined ortho-para fraction is not considered for the fitting processes. Thus, the systematic effect of a changing temperature can be neglected.

### Flow

The flow controller RF001 is a Bronkhorst®<sup>2</sup> F-201CV 20 K sensor type based on heat capacity measurement, regulating an internal automatic valve to reach the set point. However, in the experimental example shown here we only used it to measure the flow. As such, the instability in the flow rate is from the fact that at a lower catalyst temperature the pressure in the loop decreases, reducing the pumping speed and thereby the flow rate in the loop.

Since ortho and para hydrogen have different heat capacities, a correction term is needed. Bronkhorst provides a well proven correction term  $F_{mix}$

$$F_{mix} = \left( \frac{x_o}{F_o} - \frac{x_p}{F_p} \right)^{-1} \quad (2)$$

with  $x_i$  as the concentrations and  $F_i$  as the correction factors for pure ortho and pure para hydrogen.  $F_i$  is given by

$$F_i = \frac{c_{p,H_2} \cdot \rho_{H_2}}{c_{p,i} \cdot \rho_i} \quad (3)$$

with the specific heat capacities  $c_p$  at working temperature plus 50 °C and the densities  $\rho$  at 0 °C and 1013.25 mbar. This information is based on personal communication with Bronkhorst. The working temperature of 50 °C is chosen for three reasons. First, a temperature regulated sensor will be more stable than one operated at room temperature that follows temperature fluctuations in the laboratory. Second, the difference in heat capacity for ortho and para hydrogen

vanishes with increasing temperature. Third, the deviation of the real from the ideal ratio 1:3 also vanishes with higher temperatures. Nevertheless, a comparison of corrected ( $F_{mix}$ ) and uncorrected flow ( $F$ ) data shows a maximum absolute deviation of 1.5 sccm at a flow of 300 sccm leading to a relative change below 0.5% which is negligible. In comparison to that, the combined uncertainty of systematic and statistical uncertainty of the controller is 1%. In the present setup the flow is always measured in a room temperature gas stream. However, the Raman spectroscopy system provides an independent ortho-para measurement we can check its influence on the flow measurement in the data analysis.

Due to the small amount of catalyst used in the converter, the ortho-para ratio is almost identical across the whole loop and the change per measurement point (every minute) is quite small. This allows the implementation of a correction factor from the Raman measurement to the flow controller set point if needed.

### Catalyst material

To fully understand the catalysis process, a full characterization of the catalyst is needed. This includes three categories of properties. First, porosity or grain size. Second, the history of the material e.g., previous exposure and the activation procedure and process properties. Third, such as surface or transport mechanisms which will be still mandatory as accompanying experiments for model building. However, our approach can be used to test catalysis material under realistic conditions, close to those of a hydrogen liquefaction plant. For this technical application, it is sufficient to understand the integral catalytic efficiency in dependence of macroscopic parameters such as temperature, pressure, and flow.

### Setup

The whole setup including all pipes and the main components has its own systematic influence. Processes, such as back diffusion are assumed to have an impact on the catalysis process since some molecules stay longer in the converter and therefore have a higher probability to be catalysed. Therefore, we minimized dead ends in the loop and the catalyst to a minimum. We also tested this by adding a deuterium batch to a hydrogen filled loop and found that we were able to see the deuterium batch in the system for more than 10.

Full circles before it was evenly distributed in the loop. However, this is mainly relevant for the comparison with other measurement methods, since all catalysts characterised with this apparatus will suffer from the same systematics.

## Discussion & conclusion

The method presented uses Raman spectroscopy and therefore measures the ortho-para ratio directly and independent of other parameters, such as the gas temperature, flow rate and pressure. This is an inherent advantage over other methods which are based on heat capacity, heat conductivity or ortho-para conversion and rely on a complete transfer of the heat to the measurement cell and stable temperature conditions.

<sup>2</sup> registered office: AK Ruurl, Netherlands.

Methods relying in the released energy of the ortho-para conversion will not be able to see a difference close to equilibrium since the amount of released energy decreases close to the equilibrium. Methods based on speed of sound [52] strongly rely on the purity of the gas and already small contributions of other gases such as nitrogen, oxygen or helium will ruin the measurement. This makes it close to impossible to study the influence of those gases on the catalysis process. Indirect methods always depend on at least one additional parameter and therefore extensive calibration is mandatory [53].

By the use of a closed loop and cyclical operation we can use small amounts of catalyst materials, which helps for studies that will use many different and/or expensive materials. In addition, by changing the catalyst amount, we can influence the sensitivity of our measurement procedure and check for systematic effects. Also, by going to a slow conversion process, the measurement can be done very accurately, and therefore is sensitive to small effects. For example, doping the gas with impurities like nitrogen and oxygen as it might happen in technical applications by leakage. The slow conversion process also helps to achieve a good temperature homogeneity along the catalyst material, since the released heat from the ortho-para conversion can be extracted easily. Another advantage is that we can run the experiment until the low temperature equilibrium is achieved. In addition, we can also study the back conversion at a different temperature which is not possible with single pass experiments. Measurements of the equilibrium state itself also contain information about catalyst properties, which is at single pass experiments only possible with huge amounts of catalyst. For example, gas chromatography effects which can be sensitive to the ortho-para state, can influence the catalytic equilibrium and will differ to the pure gas equilibrium. This contains more information about the underlying catalytic process and helps in modelling of the microscopic process.

However, there are also disadvantages. To extract the conversion rate depending on the temperature, it is mandatory to cool down or warm up and reach homogeneous temperature distribution along the catalyst as fast as possible. Data gathered during the cool down process has to be excluded or it will change the result.

There is a trade-off between accuracy and measurement time which can be controlled by the amount of catalyst used.

If a fast scanning of a huge parameter space is needed, our apparatus can also be used in a single pass way. For this purpose, more catalyst material is put into the converter to increase the conversion rate. Gas is then sent from gas bottle or a buffer vessel to the converter. The ortho-para ratio is measured behind the converter with Raman spectroscopy and the gas is released to the stack. Thus, the advantage of quick parameter studies, such as temperature and flow dependency of the conversion efficiency of the catalyst can be combined with the benefit of a direct ortho-para measurement.

Based on our measurements, we conclude that this measurement setup is suitable to characterize materials for the use as ortho-para catalysts in dependence of macroscopic parameters, such as temperature, flow rate and pressure. The direct ortho-para measurement with Raman spectroscopy presents a substantial advantage over other existing methods since it is independent of those parameters.

The cyclical Raman approach delivers additional information, such as the ortho-para equilibrium and the reaction order which might be influenced by the catalysis process. The system can be used in a single path configuration for quick parameter studies. To summarize, this experimental device is very versatile machine for ortho-para catalysis studies with many advantages.

For our own application we could demonstrate the inline and real time monitoring and manipulation of the ortho-para ratio for the production of samples for IR-absorption and many other applications [16].

The authors acknowledge the support by the whole Tritium Laboratory Karlsruhe and especially for Tobias Weber, Nancy Tuchscherer and Albert Braun during the construction and commissioning of the setup and the support of Alexander Marsteller for internal review of the paper. We acknowledge support by the KIT- Publication Fund of the Karlsruhe Institute of Technology.

### Declaration of competing interest

The authors declare that they have no known competing financial interests or personal relationships that could have appeared to influence the work reported in this paper.

### REFERENCES

- [1] Ball M, Wietschel M. The future of hydrogen - opportunities and challenges. *Int J Hydrogen Energy* 2009;34(2):615–27. <https://doi.org/10.1016/j.ijhydene.2008.11.014>.
- [2] Marbán G, Valdés-Solís T. Towards the hydrogen economy? *Int J Hydrogen Energy* 2007;32(12):1625–37. <https://doi.org/10.1016/j.ijhydene.2006.12.017>.
- [3] Dunn S. Hydrogen futures: toward a sustainable energy system. *Int J Hydrogen Energy* 2002;27(3):235–64. [https://doi.org/10.1016/s0360-3199\(01\)00131-8](https://doi.org/10.1016/s0360-3199(01)00131-8).
- [4] Pawelczyk E, L- ukasik N, Wysocka I, Rogala A, G,ebicki J. Recent progress on hydrogen storage and production using chemical hydrogen carriers. *Energies* 2022;15(14):4964. <https://doi.org/10.3390/en15144964>.
- [5] Massarweh O, Al-khuzaei M, Al-Shafi M, Bicer Y, Abushaikha AS. Blue hydrogen production from natural gas reservoirs: a review of application and feasibility. *J CO2 Util* 2023;70:102438. <https://doi.org/10.1016/j.jcou.2023.102438>.
- [6] Zhang T, Uratani J, Huang Y, Xu L, Griffiths S, Ding Y. Hydrogen liquefaction and storage: recent progress and perspectives. *Renew Sustain Energy Rev* 2023;176:113204. <https://doi.org/10.1016/j.rser.2023.113204>.
- [7] Ringner J, Klaus M, Jurns J, Befßler Y, Lyngh D. Liquid hydrogen for cold neutron production at european spallation source ERIC. *J Phys Conf* 2018;1021. <https://doi.org/10.1088/1742-6596/1021/1/012078>. 012078.
- [8] Heisenberg W. Mehrkörperproblem und resonanz in der quantenmechanik. *Zeitschrift für Physik* 1926;38(6–7):411–26. <https://doi.org/10.1007/bf01397160>.
- [9] Hund F. Zur deutung der molekelspektren. III. *Zeitschrift für Physik* 1927;43(11–12):805–26. <https://doi.org/10.1007/bf01397249>.
- [10] Doss N, Tennyson J, Saenz A, Jonsell S. Molecular effects in investigations of tritium molecule  $\beta$  decay endpoint



- experiments. *Phys Rev C* 2006;73(2). <https://doi.org/10.1103/physrevc.73.025502>. 025502.
- [11] Saenz A, Froelich P. Effect of final-state interactions in allowed  $\beta$  decays. II. reliability of the  $\beta$ -decay spectrum for T2. *Phys Rev C* 1997;56(4):2162–84. <https://doi.org/10.1103/physrevc.56.2162>.
- [12] Große R, Beck A, Bornschein B, Fischer S, Kraus A, Mirz S, Rupp S. First calibration measurements of an FTIR absorption spectroscopy system for liquid hydrogen isotopologues for the isotope separation system of fusion power plants. *Fusion Sci Technol* 2015;67(2):357–60. <https://doi.org/10.13182/fst14-t29>.
- [13] Große R, Kraus A, Mirz S, Wozniowski S. First calibration of an IR absorption spectroscopy system for the measurement of H<sub>2</sub>, D<sub>2</sub>, and HD concentration in the liquid phase. *Fusion Sci Technol* 2017;71(3):369–74. <https://doi.org/10.1080/15361055.2017.1291237>.
- [14] Krasch B, Große R, Kuntz D, Mirz S. Design of a cryostat for spectroscopic investigation of all hydrogen isotopologues in the solid, liquid, and gaseous phases. *Fusion Sci Technol* 2020;76(4):481–7. <https://doi.org/10.1080/15361055.2020.1718841>.
- [15] Mirz S, Brunst T, Große R, Krasch B. Concentrated nonequilibrium HD for the cross calibration of hydrogen isotopologue analytics. *Fusion Sci Technol* 2020;76(3):284–90. <https://doi.org/10.1080/15361055.2020.1711688>.
- [16] Grösse R, Bornschein B, Kraus A, Mirz S, Wozniowski S. Minimal and complete set of descriptors for IR-absorption spectra of liquid H<sub>2</sub>–D<sub>2</sub> mixtures. *AIP Adv* 2020;10(5). <https://doi.org/10.1063/1.5111000>. 055108.
- [17] Cristescu I, Bükki-Deme A, Carr R, Gramlich N, Groessle R, Melzer C, Schaefer P, Welte S. Review of the tlk activities related to water detritiation, isotope separation based on cryogenic distillation and development of barriers against tritium permeation. *Fusion Sci Technol* 2017;71(3):225–30. <https://doi.org/10.1080/15361055.2017.1288057>.
- [18] Bracha M, Lorenz G, Patzelt A, Wanner M. Large-scale hydrogen liquefaction in Germany. *Int J Hydrogen Energy* 1994;19(1):53–9. [https://doi.org/10.1016/0360-3199\(94\)90177-5](https://doi.org/10.1016/0360-3199(94)90177-5).
- [19] Ohlig K, Decker L. Hydrogen, 4. liquefaction. sep 2013. [https://doi.org/10.1002/14356007.o13\\_o05.pub2](https://doi.org/10.1002/14356007.o13_o05.pub2).
- [20] Ohlig K, Decker L. The latest developments and outlook for hydrogen liquefaction technology. In: AIP conference proceedings. AIP Publishing LLC; 2014. <https://doi.org/10.1063/1.4860858>.
- [21] Cardella U, Decker L, Klein H. Economically viable large-scale hydrogen liquefaction. *IOP Conf Ser Mater Sci Eng* 2017;171. <https://doi.org/10.1088/1757-899x/171/1/012013>. 012013.
- [22] Quack H. Conceptual design of a high efficiency large capacity hydrogen liquefier. In: AIP conference proceedings. AIP; 2002. <https://doi.org/10.1063/1.1472029>.
- [23] Berstad DO, Stang JH, Neksa P. Large-scale hydrogen liquefier utilising mixed-refrigerant pre-cooling. *Int J Hydrogen Energy* 2010;35(10):4512–23. <https://doi.org/10.1016/j.ijhydene.2010.02.001>.
- [24] Wilhelmsen Ø, Berstad D, Aasen A, Neksa P, Skaugen G. Reducing the exergy destruction in the cryogenic heat exchangers of hydrogen liquefaction processes. *Int J Hydrogen Energy* 2018. <https://doi.org/10.1016/j.ijhydene.2018.01.094>. URL, <http://www.sciencedirect.com/science/article/pii/S0360319918301691>.
- [25] Berstad DO, Stang JH, Neksa P. Comparison criteria for large-scale hydrogen liquefaction processes. *Int J Hydrogen Energy* 2009;34(3):1560–8. cited By :19.
- [26] Yin L, Ju Y. Review on the design and optimization of hydrogen liquefaction processes. *Front Energy* 2019;14(3):530–44. <https://doi.org/10.1007/s11708-019-0657-4>.
- [27] Pauling L, Wilson E. Introduction to quantum mechanics: with applications to chemistry. Dover Books on Physics, Dover Publications; 1985. URL, <https://books.google.de/books?id=D48aGQTkflgC>.
- [28] Souers P. Hydrogen properties for fusion energy. Berkeley: University of California Press; 1986. URL, <http://books.google.de/books?id=I2K6DKA1IMwC>.
- [29] Hertel IV. *Atome, Moleküle und optische Physik 2: moleküle und Photonen - spektroskopie und Stre- uphysik. Bücher: Springer-Lehrbuch Springer Link*; 2010. Springer Berlin Heidelberg, Berlin, Heidelberg.
- [30] Buntkowsky G, Walaszek B, Adamczyk A, Xu Y, Limbach H-H, Chaudret B. Mechanism of nuclear spin initiated para-h<sub>2</sub> to ortho-h<sub>2</sub> conversion. *Phys Chem Chem Phys* 2006;8:1929–35. <https://doi.org/10.1039/B601594H>.
- [31] Larsen AH, Simon FE, Swenson CA. The rate of evaporation of liquid hydrogen due to the ortho-para hydrogen conversion. *Rev Sci Instrum* 1948;19(4):266–9. doi:10.1063/1.1741241. URL, <http://link.aip.org/link/?RSI/19/266/1>.
- [32] Milenko YY, Sibileva RM. Natural ortho-para conversion rate in liquid and gaseous hydrogen. *J Low Temp Phys* 1997;107(12):77–92. <https://doi.org/10.1007/BF02396837>.
- [33] Petitpas G, Aceves SM, Matthews MJ, Smith JR. Para-h<sub>2</sub> to ortho-h<sub>2</sub> conversion in a full-scale automotive cryogenic pressurized hydrogen storage up to 345 bar. *Int J Hydrogen Energy* 2014;39(12):6533–47. <https://doi.org/10.1016/j.ijhydene.2014.01.205>. URL, <http://www.sciencedirect.com/science/article/pii/S036031991400319X>.
- [34] Essler J. *Physikalische und technische aspekte der ortho-para-umwandlung von wasserstoff*. Dresden: Ph.D. thesis, Technischen Universität Dresden; 2013.
- [35] Lemmon EW, Bell IH, Huber ML, McLinden MO. Nist reference fluid thermodynamic and transport properties database (refprop) version 10 - srd 23. 2018. <https://doi.org/10.18434/T4/1502528>.
- [36] Ulucan TH, Akhade SA, Ambalakatte A, Autrey T, Cairns A, Chen P, Cho YW, Gallucci F, Gao W, Grinderslev JB, Grubel K, Jensen TR, de Jongh PE, Kothandaraman J, Lamb KE, Lee Y-S, Makhoulfi C, Ngene P, Olivier P, Webb CJ, Wegman B, Wood BC, Weidenthaler C. Hydrogen storage in liquid hydrogen carriers: recent activities and new trends. *Prog Energy* 2023;5(1):012004. <https://doi.org/10.1088/2516-1083/acac5c>.
- [37] Hall WK. Catalytic function of hydrogen bound to surfaces of oxides. *Acc Chem Res* 1975;8(8):257–63.
- [38] Minaev BF, Aagren H. Spin catalysis of ortho-para hydrogen conversion. *J Phys Chem* 1995;99(21):8936–40. <https://doi.org/10.1021/j100021a071>.
- [39] Riaz A, Qyyum MA, Hussain A, Lee M. Significance of ortho-para hydrogen conversion in the performance of hydrogen liquefaction process. *Int J Hydrogen Energy* oct 2022. <https://doi.org/10.1016/j.ijhydene.2022.09.022>.
- [40] O'Neill KT, Ghafri SA, da Silva Falco B, Tang L, Kozielski K, Johns ML. Hydrogen ortho- para conversion: process sensitivities and optimisation. *Chem Eng Process- Process Intensif* 2023;184:109272. <https://doi.org/10.1016/j.cep.2023.109272>.
- [41] Weitzel DH, Loebenstein WV, Draper JW, Park OE. Ortho-para catalysis in liquid-hydrogen production. *J Res Natl Bur Stand* 1958;60(3):221–7. <https://doi.org/10.6028/jres.060.026>.
- [42] Boeva OA, Odintzov AA, Solovov RD, Abkhalimov EV, Zhavoronkova KN, Ershov BG. Low-temperature ortho–para hydrogen conversion catalyzed by gold nanoparticles: particle size does not affect the rate. *Int J Hydrogen Energy* 2017;42(36):22897–902. <https://doi.org/10.1016/j.ijhydene.2017.07.187>. URL, <http://www.sciencedirect.com/science/article/pii/S0360319917330239>.

- [43] Knopp G, Kirch K, Beaud P, Mishima K, Spitzer H, Radi P, Tulej M, Gerber T. Determination of the ortho-/para deuterium concentration ratio with femtosecond cars. *J Raman Spectrosc* 2003;34(12):989–93. <https://doi.org/10.1002/jrs.1091>.
- [44] Long D. *The Raman effect: a unified treatment of the theory of Raman scattering by molecules*. Wiley; 2002. [http://books.google.de/books?id=Y1TVe5BdK\\_UC](http://books.google.de/books?id=Y1TVe5BdK_UC).
- [45] Schwartz C, Le Roy RJ. Nonadiabatic eigenvalues and adiabatic matrix elements for all isotopes of diatomic hydrogen. *J Mol Spectrosc* 1987;121(2):420–39. [https://doi.org/10.1016/0022-2852\(87\)90059-2](https://doi.org/10.1016/0022-2852(87)90059-2). URL, <http://www.sciencedirect.com/science/article/pii/0022285287900592>.
- [46] Le Roy RJ. Recalculation of Raman transition matrix elements of all hydrogen isotopologues for 532nm laser excitation. personal communication; 2011.
- [47] Schlosser M, James TM, Fischer S, Lewis RJ, Bornschein B, Telle HH. Evaluation method for Raman depolarization measurements including geometrical effects and polarization aberrations. *J Raman Spectrosc* 2013;44(3):453–62. <https://doi.org/10.1002/jrs.4201>.
- [48] James TM, Schlosser M, Lewis RJ, Fischer S, Bornschein B, Telle HH. Automated quantitative spectroscopic analysis combining background subtraction, cosmic ray removal, and peak fitting. *Appl Spectrosc* 2013;67(8):949–59. <https://doi.org/10.1366/12-06766>.
- [49] Schlosser M, Rupp S, Brunst T, James TM. Relative intensity correction of Raman systems with national institute of standards and technology standard reference material 2242 in 90°-scattering geometry. *Appl Spectrosc* 2015;69(5):597–607. <https://doi.org/10.1366/14-07748>.
- [50] Huber KP, Herzberg G. *Molecular spectra and molecular structure: IV. Constants of diatomic molecules*. Van Nostrand Reinhold Company; 1979.
- [51] Bachmann L. Gas-chromatographic separation of ortho- and parahydrogen on molecular sieves: analysis, preparation, and measurement of catalytic conversion and of adsorption. *J Catal* 1962;1(2):113–20. [https://doi.org/10.1016/0021-9517\(62\)90015-5](https://doi.org/10.1016/0021-9517(62)90015-5).
- [52] Eisenhut S, Klaus M, Baggemann J, Rucker U, Beßler Y, Schwab A, Haberstroh C, Cronert T, Gutberlet T, Brückel T, Lange C. Cryostat for the provision of liquid hydrogen with a variable ortho- para ratio for a low-dimensional cold neutron moderator. *EPJ Web Conf* 2020;231. <https://doi.org/10.1051/epjconf/202023104001>. 04001.
- [53] Essler J, Haberstroh C. Performance of an ortho-para concentration measurement cryostat for hydrogen. In: *AIP conference proceedings*. AIP; 2012. <https://doi.org/10.1063/1.4707124>.